31st Annual International Conference of the IEEE EMBS
Minneapolis, Minnesota, USA, September 2-6, 2009

4D CT Image Simulation Using B-Spline Deformable Model and Cosine Interpolation of Deformation field

Zhen Tian, Kehong Yuan and Yanling Bai

Abstract— **Four-dimensional computed tomography(4D CT) is significant in radiotherapy treatment planning for thorax and upper abdomen to take their motion induced by respiration into consideration, but its high radiation dose becomes a major concern and impedes its wide application. To solve the problem, we propose an image interpolation approach to get 4D CT simulation images. We simulate 4D CT images at arbitrary intermediate phases by B-Spline deformable model with cosine interpolation of the deformation field, which is obtained by deformable registration of two CT images at end-exhale and end-inhale phases. The mean of absolute differences computed between actual 4D CT images and simulation ones is used to evaluate the accuracy of simulation. Our experiment results show that both linear interpolation and cosine interpolation with proper parameters perform well and the latter performs a little better than the former in general.**

I. INTRODUCTION

Respiratory motion induces significant movements of thoracic and abdominal tumors which pose a great challenge in thorax and abdomen radiotherapy planning and delivery, leading to image artifacts [1] and distorted target volume [2], making target site under-irradiated and healthy tissues unnecessarily irradiated. Breath-hold and respiratory gating have mainly been employed to handle the tumor motion, in which the radiotherapy accuracy is at the cost of making patients uncomfortable or lengthening treatment time [3].

Four-dimensional computer tomography(4D CT) have been proposed to acquire a set of CT images at different respiratory phases by sorting free-breathing multi-slice CT scans and reconstructing them into phase-binned images [4]. Although 4D CT has been reported to successfully account for respiratory motion in images [5], its high radiation dose to patients becomes a major concern and impedes its wide clinical application. In axial cine mode, data acquisition is implemented at least in one respiratory cycle for every couch position and about 10 20 sets of phase-resolved 3D CT images are acquired, which means a huge increase of radiation dose. Therefore effective dose reduction is highly desirable for clinical application of 4DCT.

A novel method has been reported to perform 4D scan at a lower current to reduce the patient radiation dose [6], in which a sophisticated smoothing algorithm is needed to deal with the increased statistical noise caused by the low current. Another method reported is to simulate 4DCT images with two regular CT images at end-exhale and end-inhale phases [7], [8]. Deformable registration is used to study the correlation between these two phases and obtain the deformation field. 4D CT images at intermediate phases are deduced by a deformable model with linear interpolation of the deformation field. This method not only greatly reduces the radiation dose required for 4D CT, but also avoid the artifacts of actual 4D CT images if the correlation between external respiratory signal and scanner is not accurate. Besides, this method breaks up the limitation of time resolution of actual 4D CT permits and permits us to obtain images at arbitrary phases. The majority of studies on this method mainly focused on image registration, and they didn't pay much attention to another important part of 4D CT images simulation: image interpolation, that is, to deduce simulation images with deformable model and interpolation of deformation field. Linear interpolation, which is based on the supposition that lung motion is linear and uniform, was usually used to get intermediate deformation field for warping image with deformable model.

In our paper, we take the change of lung motion speed into consideration and use cosine interpolation to interpolate the deformation field between CT images at end-exhale and end-inhale phases by a modified cosine signal representing respiratory motion to estimate deformation fields for intermediate phases. Then a B-Spline deformable model is used to deduce 4D CT simulation images at intermediate phases with these deformation fields. The performance of simulation is evaluated by the mean of absolute differences between actual images and simulation ones. The results of cosine interpolation are compared with that of linear interpolation to see whether it performs better or not.

II. METHODS AND MATERIALS

A. Image Acquisition

Only two regular 3D CT images at end-exhale and end-inhale phases are needed to get simulation images of 4D CT. However, here, in order to better evaluate the performance of 4D CT simulation, three 4D CT lung cases were acquired by Philips Brilliance CT BigBore scanner with 5mm slice thickness. The number of slice images in these cases were 43, 49 and 52 respectively and these images were all 512×512 in size and in DICOM image format. Eight respiratory phase bins were set for the 4D study which were indexed from CT0 to CT70, with CT0 corresponding to the starting phase of inspiration and CT30 the full inspiration phase. CT0 to

This work was supported by the Scientific and Technological Planning Program of Guangdong Province of China (Grant No. 2008B030303055), and the Scientific and Technological Planning Program of Heilongjiang Province of China (Grant No. GZ05C402).

Z. Tian and K.Yuan are with Faculty of Graduate School at Shenzhen and Department of Biomedical Engineering, Tsinghua University,China yuankh@sz.tsinghua.edu.cn

Y. Bai is with Tumor Hospital, Harbin Medical University, Harbin 150086, China

CT30 represent inspiration while CT40 to CT70 represent expiration.

Here, we regard the two image sets of CT0 and CT30 as the regular 3D CT images at end-exhale and end-inhale phases. The actual CT10, CT20 images are used to make a comparison with simulation images of corresponding phases to evaluate the performance of our approach.

B. Image Preprocessing

The registration algorithm used in our study is voxel-based and vulnerable to image noise. Therefore, anisotropic diffusion is used in image preprocessing for denoising, by which noise is reduced and texture is preserved and enhanced. The motivation for anisotropic diffusion is that a Gaussian smoothed image is a single time slice of the solution to the heat equation, that has the original image as its initial conditions. It includes a variable conductance to limit the smoothing at edges and a time parameter which represents the effective width of the filter when using Gaussian kernels. More information about anisotropic diffusion can be found in [9].

Besides, the deformable registration used in the next step is based on the assumption that for every point, its intensity is conserved from the fixed image to the floating one but at a different location. However, this intensity conservation assumption is invalid inside the lung where the changing quantity of inspired air leads to change of voxel intensity. Therefore, lung intensity is artificially modified to make sure the intensity conservation between two sets of registration images. Here, region growing algorithm [10] is used to segment the lung out and calculate the mean lung intensity. Let I_1 and I_2 be the two images to be registered, ρ_1 and ρ_2 denote the mean of lung intensity of the two images. We artificially modify the intensity value $I_1(x)$ of point x which is inside of lung by $I_1'(x) = I_1(x) + \rho_2 - \rho_1$.

C. Image Deformable Registration

Here image deformable registration is to register the two CT images CT0 and CT30 to get their deformation field for image interpolation in the next step. In our study, B-Spline deformable model [11] is used in image non-grid registration because of its simplicity. The model only uses a lattice of nodes overlaid on the image, and deformation at any other location in the image is deduced by spline interpolation of deformation coefficients of close nodes. Therefore, the B-Spline model is locally controlled, that is, the displacement of a point can only be influenced by its close nodes. Here, CT0 was set to be fixed image I_a and CT30 floating image I_b. The image is divided into a grid with N^3 nodes.

In our study, we use a lattice of 18 nodes for each dimension in image registration with a B-Spline deformable model. Because each node has three variables representing the displacements in three different directions, therefore there are 6591 variables that need optimizing to find the minimum of the registration metric. Here, limited memory Broyden, Fletcher, Goldfarb and Shannon algorithm (LBFGS), which is good at dealing with high-dimensional optimization problems, is adopted to minimize registration metric [12]. Here, we use normalized cross correlation (NCC) between two images as the registration metric. The calculation of NCC is as follows:

$$NCC = \frac{\sum_{i=1}^{N^3}(I_a(x_i) - I_{a0})(I_b(Tx_i)) - I_{b0})}{\sqrt{\sum_{i=1}^{N^3}(I_a(x_i) - I_{a0})^2 \sum_{j=1}^{N^3}(I_b(Tx_j) - I_{b0})^2}} \quad (1)$$

$$I_{a0} = \frac{1}{N^3}\sum_{i=1}^{N^3} I_a(x_i) \quad (2)$$

$$I_{b0} = \frac{1}{N^3}\sum_{i=1}^{N^3} I_b(Tx_i) \quad (3)$$

where i and j are the node indices of fixed image, $I_a(x_i)$ is the intensity of node x_i on the fixed image I_a, and $I_b(Tx_i)$ is the intensity of mapped position of node x_i on floating image I_b.

D. Image Interpolation

Image interpolation is to deduce simulated intermediate CT images between CT0 and CT30 by warping CT30 using a B-Spline deformable model with intermediate deformation fields which are estimated by interpolation of the deformation field obtained in the last step. The deformation field derived from image registration between CT0 and CT30 denotes the displacements of each voxel in the fixed image. We suppose that each point moves along its displacement vector by a straight line. The intermediate displacement can be derived by interpolation of the whole displacement vector. Let u be the deformation field that warps image CT30 to CT0, we can obtain the intermediate deformation field by $u_s = su, s \in [0,1]$.

Although the straight line trajectory is a well approximation of motion between end-exhale and end-inhale for the majority of lung points [13], the lower-middle regions of the lungs present larger motion nonlinearity and hysteresis, which should not be neglected in the future.

Here, we use and compare two deformation field interpolation methods: linear interpolation (LI) and cosine interpolation (CI). LI supposes the moving speed of each point to be constant. However, this assumption is invalid in lung motion induced by respiratory motion. Rather than constant speed model, a modified cosine model developed by Lujan [14] is preferred to be used to describe the organ respiratory motion. The model is given by

$$x(t) = x_0 + Acos^{2n}(\pi t/\tau + \phi) \quad (4)$$

where x_0 is the position of point at the end of exhale, A is the movement amplitude, τ is the cycle of breathing and ϕ is the starting phase. The factor n alters the shape of the breathing curve, the bigger n denotes the longer time spent in exhale phase compared to the time spent in inhale. In our study, we use this modified cosine curve as the interpolation

curve to obtain the intermediate displacement for every point in the floating image. Thus $s = cos^{2n}(\pi t/\tau + \phi)$, where τ is twice of the period between CT0 and CT30, $t = 0$ denotes the end of exhale phase CT0, thus ϕ is set to be $\pi/2$, n is set to be 1 and 2 respectively in CI1 and CI2.

III. RESULTS AND DISCUSSION

In the first step of image registration, the initial values of the registration metric of these three cases are about -0.98. The convergence tolerance is set to be 10^{-6} and convergence is achieved in less than 100 iterations. The final absolute values of the registration metric are about 0.998. The result of image registration of case1 in sagittal, coronal, axial views respectively are illustrated in Fig.1. The comparison of difference images before and after registration in the last two rows proves that BSpline method can effectively model the lung respiratory motion. The residue differences between CT0 and warped CT30 are mainly due to the different intensity of blood vessel because of different filling extent.

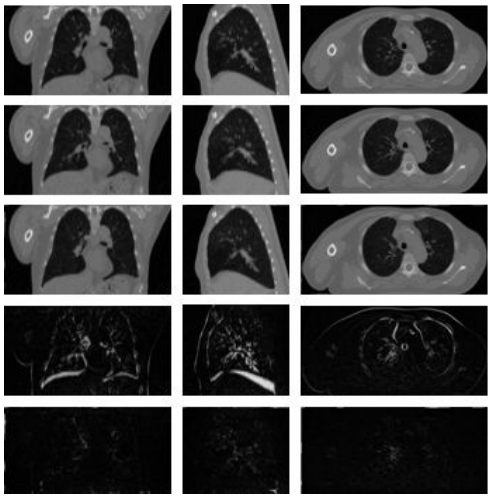

Fig. 1. The result of image deformation registration of case1: the first row shows images of CT0; the second row and third row show images of CT30 before and after deformable registration respectively; the fourth and fifth row show difference image of CT0 and CT30 before and after registration respectively; the three columns show the images in sagittal, coronal, axial views respectively.

Two deformation field interpolation algorithms (linear interpolation and cosine interpolation) are adopted and compared in our study. The actual images and simulation ones of CT20 of case1 in sagittal, coronal, axial views are shown in Fig.2. All these difference images are almost totally black, which illustrates that LI, CI1 and CI2 all perform well enough to get simulation 4D CT images. From the local amplified difference images shown in the last row, we can see that CI1 performs a litter better than LI, and CI2 performs worst.

In order to better evaluate and compare the performance of these interpolation methods, the mean of absolute differences

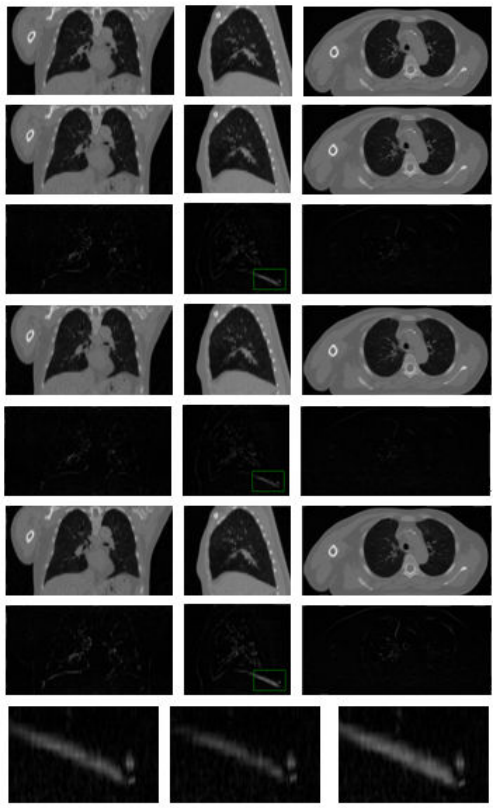

Fig. 2. The result of image interpolation of case1: the first row shows the actual CT20 images; the second, fourth, sixth rows show the simulation ones acquired by LI, CI1, CI2 respectively; the third, fifth, seventh rows show the difference image between actual and simulation images with LI, CI1, CI2 respectively; the last row shows the amplified region in green rectangle on the difference images in coronal view with LI, CI1, CI2 respectively from left to right.

(MAD) between the actual CT images and the interpolated images is calculated, which is illustrated in Fig.3. We can see from the first two subfigures that for all the three cases, LI performs a little better than CI1 in simulating CT10 images, which is converse in simulating CT20 images, and CI2 performs worst in both CT10 and CT20 simulations for all cases. The last subfigure illustrates that CI1 performs a little better than LI in general and CI2 is the worst. It is also observed that MADs of CT20 are much smaller than that of CT10.

We think that the differences between the actual CT images and interpolated simulation images are caused and influenced by three factors. One is the accuracy of image registration between images at end-exhale and end-inhale phases. The second is the different intensity of blood vessel between CT30 phases and the intermediate phases in that the simulation images are acquired by warping CT30 images with interpolated deformable field, therefore the difference could not be reduced by image registration or interpolation. The last is the difference between the real motion and the

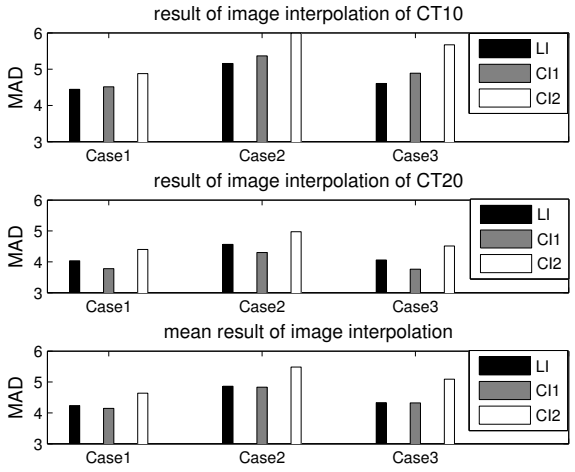

Fig. 3. MAD values of all three cases on CT10 and CT20 with LI, CI1 and CI2

motion model on which the interpolation algorithms are based, that is, how the speed changes according to the interpolation model and whether nonlinearity and hysteresis of lung motion can be ignored in a specific case. Since the interpolation algorithms use the same deformation field to get intermediate deformation field to warp image for 4D CT simulation images, the different MADs in Fig.3 reflect how the interpolation models represent the real lung motion. Therefore the results we get from Fig.3 can be explained that lung motion at the intermediate phases near to the start of inspiration (CT0) is better approximated by linear constant-speed model than cosine model, while lung motion at the intermediate phases near to the full inspiration(CT30) is better represent by cosine model of $n = 1$ with a lower speed. The result that MADs of CT20 are smaller than that of CT10 can be explained by two reasons. First, the smaller time interval between CT20 and CT30 results in smaller intensity difference of blood vessel between them; Second, the smaller time interval also results in smaller errors due to motion nonlinearity neglected in our approach.

IV. CONCLUSIONS AND FUTURE WORKS

A. Conclusions

In this paper, we get 4DCT simulation images by B-Spline deformable model and cosine interpolation of deformation field derived by image registration between CT images at end-exhale and end-inhale phases. Because the registration in our study is based on image intensity, images are pre-processed by denoising with anisotropic diffusion algorithm and modifying lung intensity artificially with image segmentation to ensure the accuracy of image registration. B-Spline deformation registration is employed and proved to be well in modeling the lung motion between end-exhale and end-inhale phases. Cosine interpolation, which is based on the straight-line trajectory assumption and the respiratory motion model proposed by Lujan, is used in our study to get intermediate deformation fields with which CT30 image is warped to obtain intermediate images. The results of our experiments show that both linear interpolation and cosine interpolation with proper parameters are well enough in simulating 4DCT images and the latter performs a bit better in general, and linear interpolation is a little better in CT10 simulation and cosine interpolation with $n = 1$ a little better in CT20, which proves that the straight-line assumption is a well approximation of lung motion and the speed at the phases near to the start of inspiration is more likely to be constant and the speed slows down at the phases near to full inspiration like the cosine model.

B. Future Works

Although the assumption that lung motion is a straight-line trajectory can well approximate the real motion for the majority of lung points, the real motion is nonlinear and subject to hysteresis, which is specific to different cases and different parts of lung. In future work, we expect to take the nonlinearity and hysteresis of lung motion especially that of the lower-middle part of lungs into consideration and propose a proper non-straight-line deformation field interpolation algorithm in order to further reduce the difference between the actual images and simulation images.

REFERENCES

[1] S. Shimuzu, H. Shirato, K. Kagei, et al, "Impact of respiratory movement on the computed tomographic images of small lung tumors in three-dimensional (3D) radiotherapy", *International Journal of Radiation Oncology Biology Physics*, vol. 46, 2000, pp 1127-1133.

[2] M. van Herk, "Errors and margins in radiotherapy", *Seminars in Radiation Oncology*, vol. 14, 2004, pp 52-64.

[3] G.S. Mageras, E. Yorke, "Deep inspiration breath hold and respiratory gating strategies for reducing organ motion in radiation treatment", *Seminars in Radiation Oncology*, vol. 14, 2004, pp 65-75.

[4] E. Rietzel, T. Pan, G.T. Chen, "Four-dimensional computed tomography: image formation and clinical protocol", *Medical Physics*, vol. 32, 2005, pp 874-889.

[5] X. Sheng, H.T. Russell, F. Gabor, et al, "Lung deformation estimation and four-dimensional CT lung reconstruction", *Academic Radiology*, vol. 13, 2006, pp 1082-1092.

[6] T. Li, E. Schreibmann, B. Thorndyke, et al, "Radiation dose reduction in four-dimensional computed tomography", *Medical Physics*, vol. 32, 2005, pp 3650-3660.

[7] E. Schreibmann, T.Y. Chen George, L. Xing, "Image interpolation in 4D CT using a BSpline deformable registration model", *International Journal of Radiation Oncology Biology Physics*, vol. 64, 2006, pp 1537-1550.

[8] Sarru David, Boldea Vlad, Miguet Serge, et al, "Simulation of four-dimensional CT images from deformable registration between inhale and exhale breath-hold CT scans", *Medical Physics*, vol. 33, 2006, pp 605-617.

[9] P. Perona, J. Malik, "Scale-space and edge detection using anisotropic diffusion", *IEEE Transactions on Pattern Analysis Machine Intelligence*, vol. 12, 1990, pp 629-639.

[10] S.A. Hojjatoleslami, J. Kittler, "Region growing: a new approach", *IEEE Transactions on Image Processing*, vol. 7, 1998, pp 1079-1084.

[11] S. Lee, G. Wolberg, K.Y. Chwa, et al, "Image metamorphosis with scattered feature constraints", *IEEE Transactions on Visualization and Computer Graphics*, vol. 2, 1996, pp 337-354.

[12] R.H. Byrd, P. Lu, J. Nocedal, et al, "A limited memory algorithm for bound constrained optimization", *SIAM Journal on Scientific and Statistical Computing*, vol. 16, 1995, pp 1190-1208.

[13] V. Boldea, C.S. Gregory, B.J. Steve, "4D-CT lung motion estimation with deformable registration: Quantification of motion nonlinearity and hysteresis", *Medical Physics*, vol. 35, 2008, pp 1008-1018.

[14] A.E. Lujan, E.W. Larsen, J.M. Balter, et al, "A method for incorporating organ motion due to breathing into 3D dose calculations", *Medical Physics*, vol. 26, 1999, pp 715-720.